

## CREWES 2018 multi-azimuth walk-away VSP field experiment

Kevin W. Hall, Kevin L. Bertram, Malcolm Bertram, Kris Innanen, and Don C. Lawton

### ABSTRACT

CREWES conducted a high-resolution multi-azimuth walk-away three-component vertical seismic profile (VSP) survey at the Containment and Monitoring Institutes Field Research Station (FRS) in the first week of September 2018. This data is primarily intended for use in full-waveform inversion (FWI) and modelling studies. The FRS has three wells, referred to here (from SW to NE) as the geophysics, injection and geochemistry wells. Four of the thirteen source lines were acquired with a 10 m VP spacing (bearings  $0^{\circ}$ ,  $45^{\circ}$ ,  $90^{\circ}$ ,  $135^{\circ}$ ), and the remainder were acquired at 60 m VP spacing. The source was an Inova Univib running a linear 1-150 Hz sweep. In addition to existing permanent 3C geophones and fibre at the FRS, High Definition Seismic Corporation deployed a string of Inova 3C VectorSeis accelerometers in the geophysics well at a nominal 1 m spacing, from the surface to 324 m depth. The data are currently undergoing zero-offset and far-offset VSP processing. First-break picks sorted by offset and azimuth appear to confirm the presence of weak HTI anisotropy at the FRS, as observed on a single offset semi-circular walk-around VSP recorded in the injection well in 2015.

### INTRODUCTION

CREWES conducted a high-resolution multi-azimuth walk-away three-component vertical seismic profile (VSP) survey and a simultaneous dual-Vibe survey at the Containment and Monitoring Institutes Field Research Station (CaMI.FRS) in the first week of September 2018. This data is primarily intended for use in full-waveform inversion (FWI) and modelling studies.

#### Source Overview

Figure 1 shows Vibe Points (VP) as red dots for thirteen source lines. Twelve source lines are centered on the geophysics well (Observation well 2) and are separated by counter-clockwise fifteen-degree rotations. Four of the source lines (lines 1,4,7 and 10), were acquired at a 10 m VP spacing and the others were acquired at 60 m spacing. The minimum source offset from the geophysics well was 6 m, and the maximum was 480 m. Note the gaps in VP coverage due to required offsets from high-pressure hydrocarbon pipelines (red lines). Source line 13 is high-lighted by blue dots representing surface 3C receiver locations for instrument testing. Some VP within 60 m of the well were dropped due to well site infrastructure. Planned VP locations in the NE quadrant inside the 60 m ring on source line 1 were rotated clockwise to source line 12, and from source line 4 counter-clockwise to source line 5. The sweep used was a low-frequency 1-150 Hz linear sweep over 16 s with 0.2 s half-cosine tapers and a 3 s listen time. Acquisition was conducted using an Inova Geophysical Univib, with two sweeps per VP.

Source line 13 was acquired with two Vibes, the Inova Univib at 40% of peak force and the University of Calgary's IVI EnviroVibe at 60% of peak force. The vibes were operated simultaneously, starting at the same time-zero, and both running a linear 10-150 Hz sweep

over 16 s with 0.2 s half-cosine tapers and a 3 s listen time. Source gathers were acquired for each Vibe separately, followed by both vibes at the same time. VP were acquired with the Vibes proceeding down the line with a fixed distance between them, and again with the Univib stationary and the EnviroVibe marching towards it. This data is addressed by Trad (2018). Permanent vertical and horizontal GPUSA Vibratory sources were also tested (Spackman, 2018), running a 0 to 100 Hz sweep that lingered at 100 Hz before running back down to 0 Hz, over 55 s.

### **Receiver Overview**

The Cami.FRS has a permanent buried 5 km optical fibre loop in place. The loop runs 1) down and back up the geophysics well with straight fibre, 2) down and back up the geophysics well with experimental helically wound fibre, 3) down and back up the geochemistry well with straight fiber, 4) to the south end of an approximately 1 km long and 1 m deep horizontal trench with straight fiber, 5) the length of the trench with helical fiber, and 6) back along the trench to the geophysics well as straight fibre. The trenched fibre is located parallel to source line 13. All VP in the walk-away VSP were recorded on this fibre loop with a Fotech interrogator. In addition, the geophysics well has 24 permanent Geospace GS-32CT 10 Hz 3C geophones cemented into position on the outside of the casing at a 5 m interval from 195 m to 310 m, which were listened to with a Geode system.

High Definition Seismic Corporation (HDSC) deployed a string of Inova 3C VectorSeis accelerometers in the geophysics well at 1 m spacing, from the surface to about 324 m depth, recorded on an Inova Scorpion system. The 1 m spacing was achieved by interleaving separate 2 m cables. Unfortunately, one of the two deepest cables failed during deployment. Time and budget did not allow the string to be removed from the well for trouble shooting. Inclination data from the VectorSeis show that rather than being entirely vertical, the well is inclined by up to nine degrees at the deepest receiver location (Figure 2) at an unknown azimuth. Projecting measured receiver depth to true vertical depth using the measured inclinations gives us a 0.3 m vertical and 5.6 m horizontal error for the deepest receiver.

Surface receivers included a 100x100 m at 10 m receiver spacing permanent patch centred on the injection well, of Inova SM7 3C geophones buried about 1 m deep. Inova Hawk nodes were attached to these geophones and recorded all vibe points. The Hawk were left in the field for a continuous background survey for about a month after completion of the VSP. Macquet (2018) reports on research conducted on similar data acquired in 2017. Ten Hz vertical component geophones were laid out along source line 13 at a 10 m spacing and recorded on Inova (ARAM) Aries system. In addition, Inova Hawk and Quantum nodes were laid out along the same line for node and receiver tests.

This report focuses on initial zero-offset and far-offset VSP processing results for VP on source lines one through twelve recorded on the VectorSeis accelerometers in the geophysics well, as well as looking for evidence of HTI anisotropy in the direct arrival times recorded in the borehole.

Newell County 2018 TL

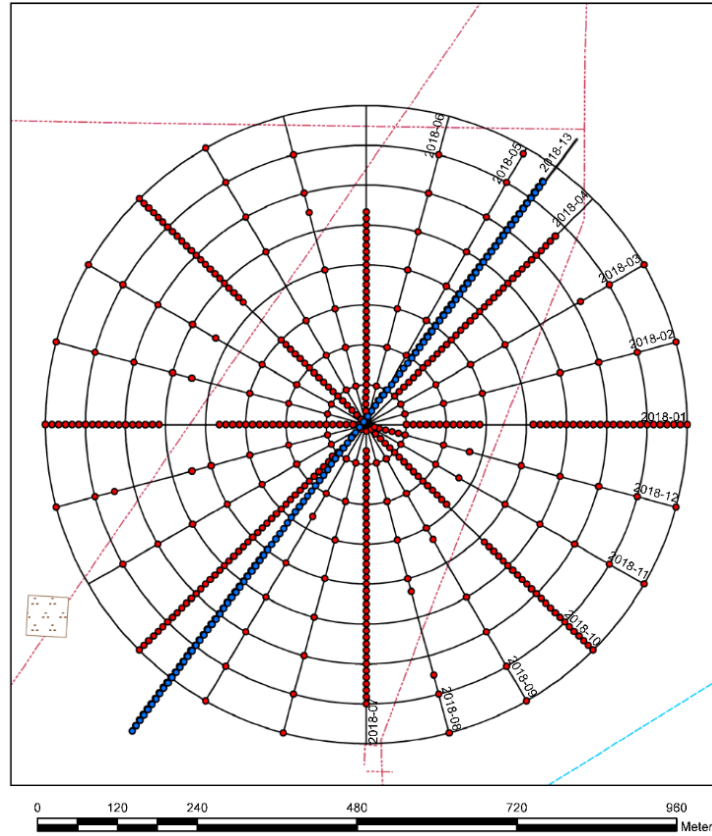


FIG. 1. Survey map. Black rings are 60 m interval circles centred on the geophysics well. Red dots are Vibe points, Blue dots are surface receiver locations, red lines are hydrocarbon pipelines.

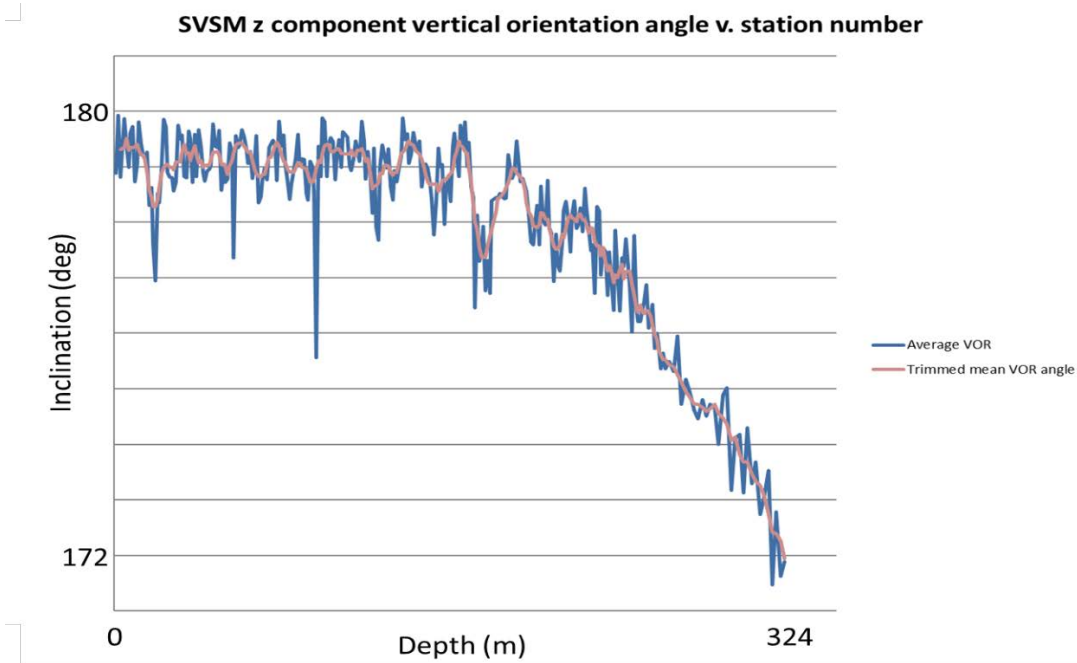


FIG. 2. Accelerometer deviation from vertical in the geophysics well. Figure courtesy of HDSC.

## SYNTHETIC SEISMOGRAMS

Figures 3 and 4 show P-P and P-S synthetic seismograms calculated using the CREWES Syngram software package for well logs recorded in the geophysics well. The  $V_p$  (blue),  $V_s$  (red) and density (green) well logs are shown on the left of each figure. The wavelet shown is the auto-correlation of the Vibe sweep used in the field. The centre of each figure displays synthetic traces calculated for 0 to 60 m source offsets from the well, which show AVO effects, at least in the P-S case, and the stack of this offset panel is shown on the right, repeated three times. A heavy black line indicates the top of the reservoir of interest, which is the basal Belly River Group sandstone. The well logs cover the bottom two thirds of the geophysics well and convert to just over 100 ms of P-P synthetic data.

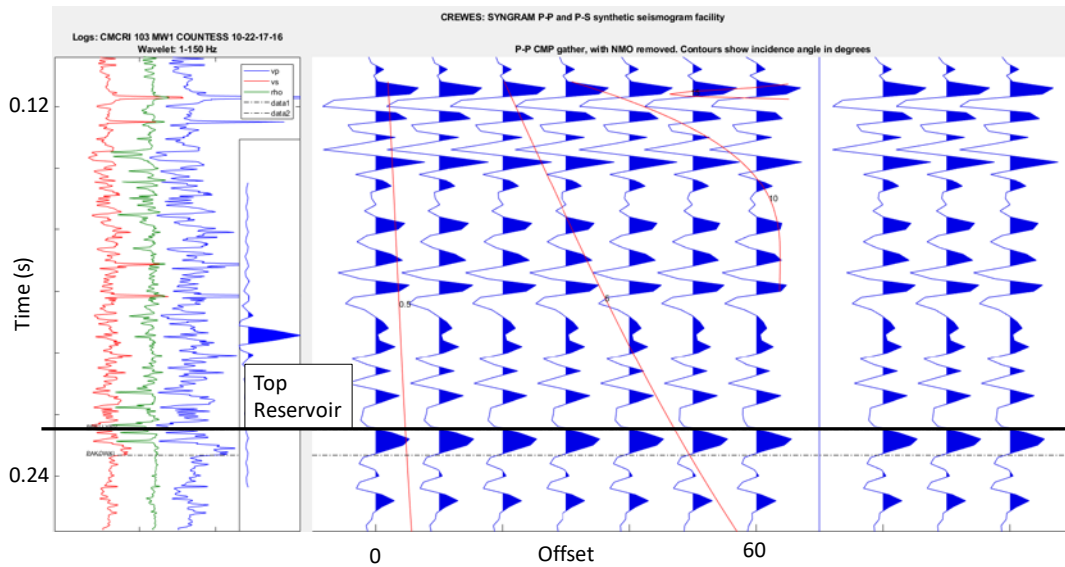


FIG. 3. P-P synthetic seismogram.

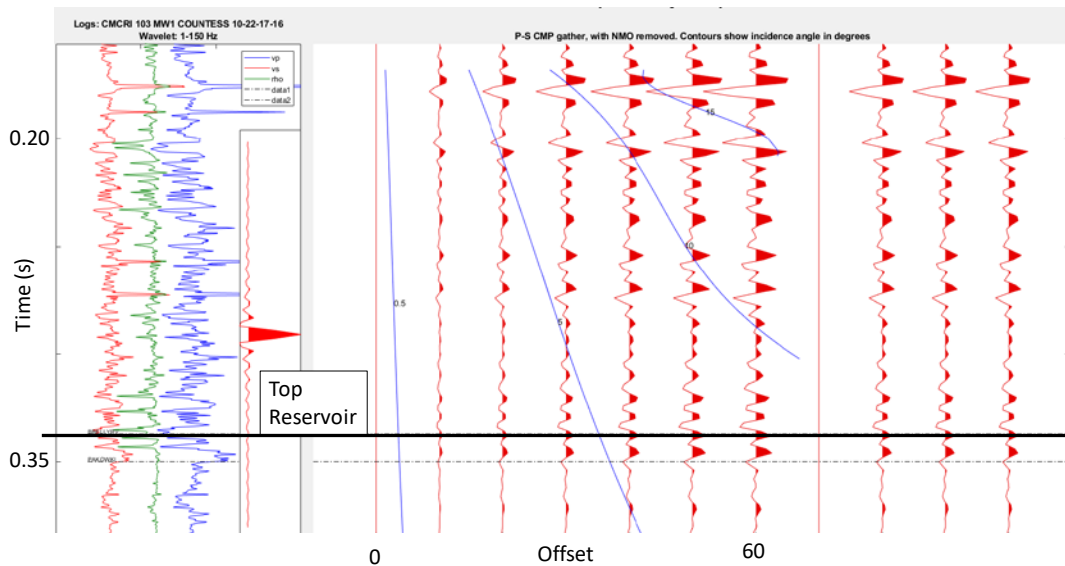


FIG. 4. P-S synthetic seismogram.

## ZERO OFFSET VSP PROCESSING

Figure 5 shows the results of wavefield separation and deconvolution for VP 1149, which is about 6 m from the geophysics well. In this case, the down-going P wave-field (P-down) was extracted from the raw vertical component data (V-row) by flattening on first-break picks and median filtering. The up-going P wave-field (P-up) was extracted by subtracting P-down from V-row, and finally was deconvolved using P-down (right-hand panel). Figure 6 shows first-break top mute and inside corridor mute after conversion to two-way travel time as well and the outside corridor stack (wiggle traces, repeated 10 times) compared to the P-P synthetic.

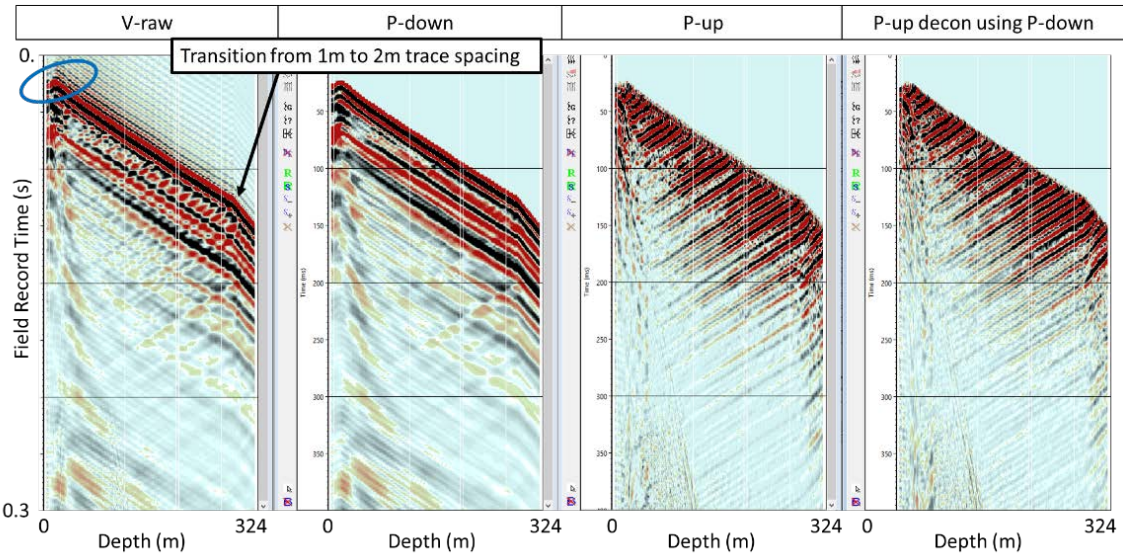


FIG. 5. Zero-offset VSP wavefield separation. Blue ellipse on V-row highlights a lack of polarity reversal on the direct arrival in the near surface.

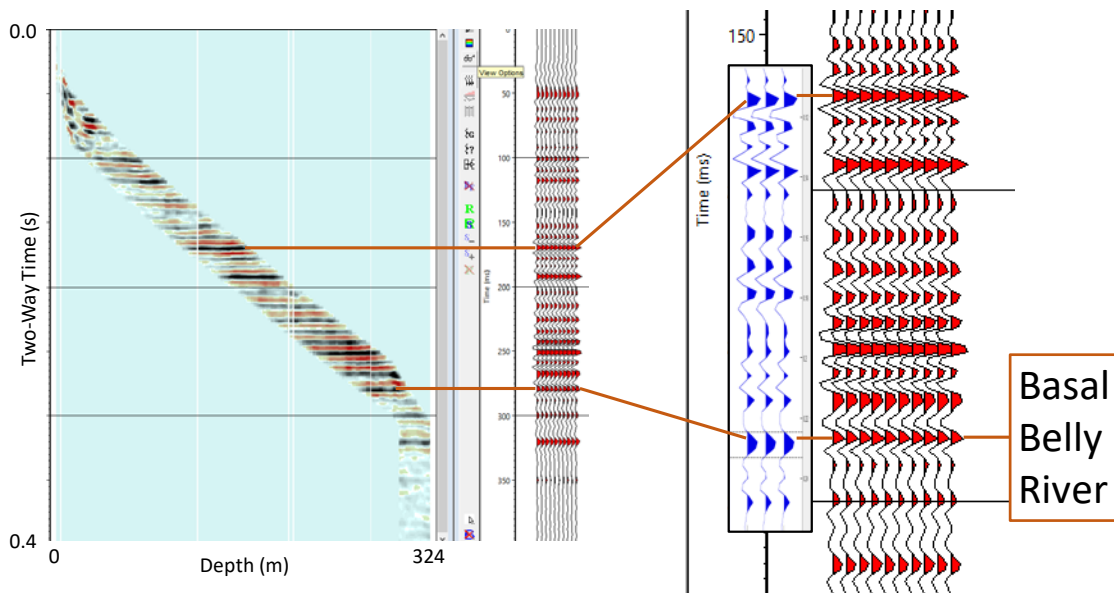


FIG. 6. Zero offset VSP corridor stack after deconvolution with down-going P-wavefield compared to P-P synthetic.

## SOURCE STATICS

We know from a previous 3C-3D survey acquired in 2014 (Isaac and Lawton, 2014) that source statics at the FRS can vary by up to 15 ms across the survey area. Figure 7 shows a map of the 2014 source refraction statics with the 2018 VP locations overlain. The source statics were interpolated, smoothed, and displayed in Matlab®. The same interpolator was then used to generate a file of source statics that could be used for processing the far offset 2018 VSP survey.

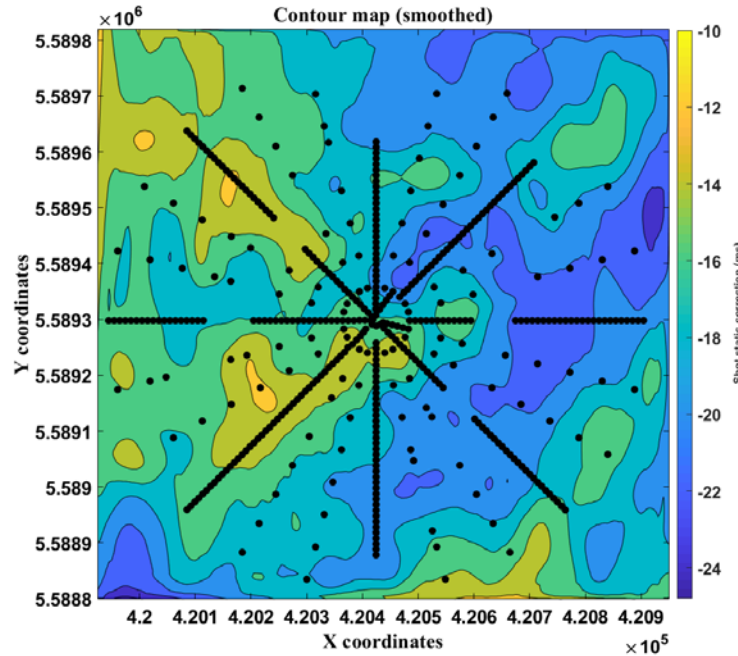


FIG. 7. 2014 3C-3D interpolated and smoothed source statics with 2018 walk-away VPs overlain.

## THE SEARCH FOR ANISOTROPY

A walk-around VSP conducted at the FRS in 2015 with a semi-circular source line at 400 m radius centred on the injection well resulted in observed travel time variations on the order of 3 ms for a single receiver at 383.5 m depth (Hall et al., 2015). The fast direction roughly coincided with source line 13 of the 2018 survey (SW-NE; see Figure 1, this report), and the fit to a 2PSI azimuthal travel-time variation model led to an interpretation of weak HTI anisotropy caused by fracturing due to the regional stress field. No source statics were applied to these data.

Figures 8 and 9 show first-break pick times from the 2018 survey displayed in constant source-receiver offset panels 60, 120, 180, 240 (top row); 300, 260, 420 and 480 (bottom row) metres, plotted against receiver depth and source-receiver azimuth. Like the 2015 survey, sinusoidal patterns can be observed in azimuth, for example, the red lines on the 240 m offset panel, Figures 8 and 9. The amplitudes of the sinusoids are greatly reduced when source statics from the 2014 3C-3D survey are applied (Figure 9). Similarly, if we position first-break times at their associated VP locations for fixed receiver depths, interpolate and contour (Figures 10 and 11), we expect non-circular contour lines if anisotropy is present (Figure 10). Application of source statics makes the contour lines

more circular (Figure 11). HTI anisotropy, while likely present, may be even weaker than previously thought. Contour lines for deeper receivers also become more circular with application of source statics, but the contours are not necessarily centred on the well location (not shown). This may be due to well deviation from vertical with depth. It will be interesting to see if this effect correlates with azimuths recorded on future dip logs.

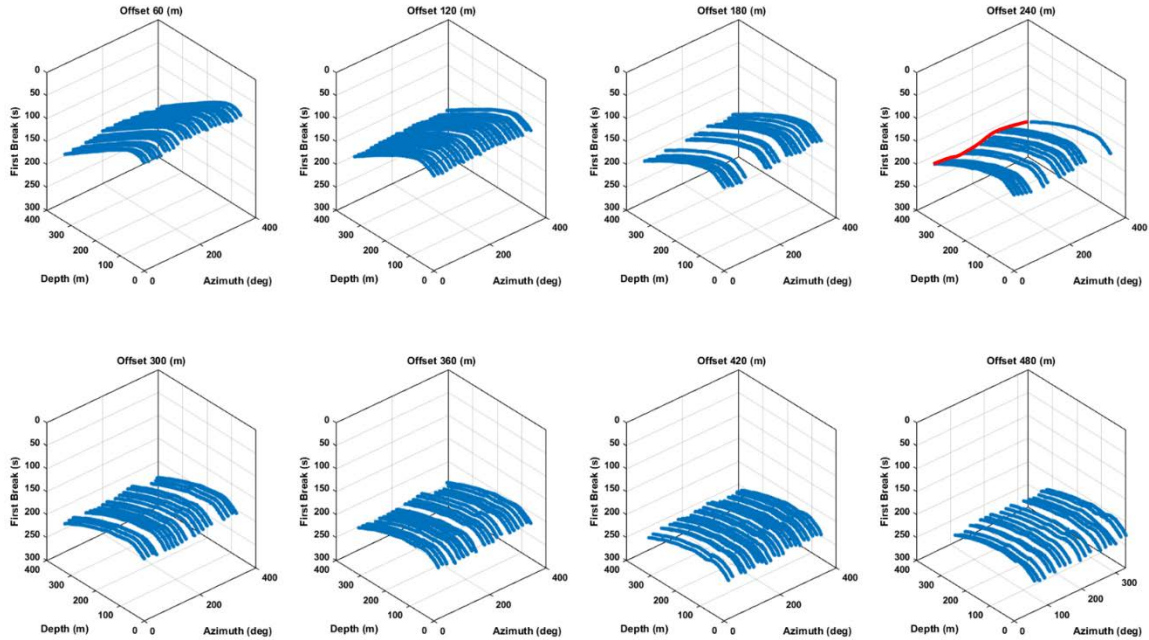


FIG. 8. Offset panels of first break picks. Sinusoidal patterns with azimuth may indicate the presence of anisotropy.

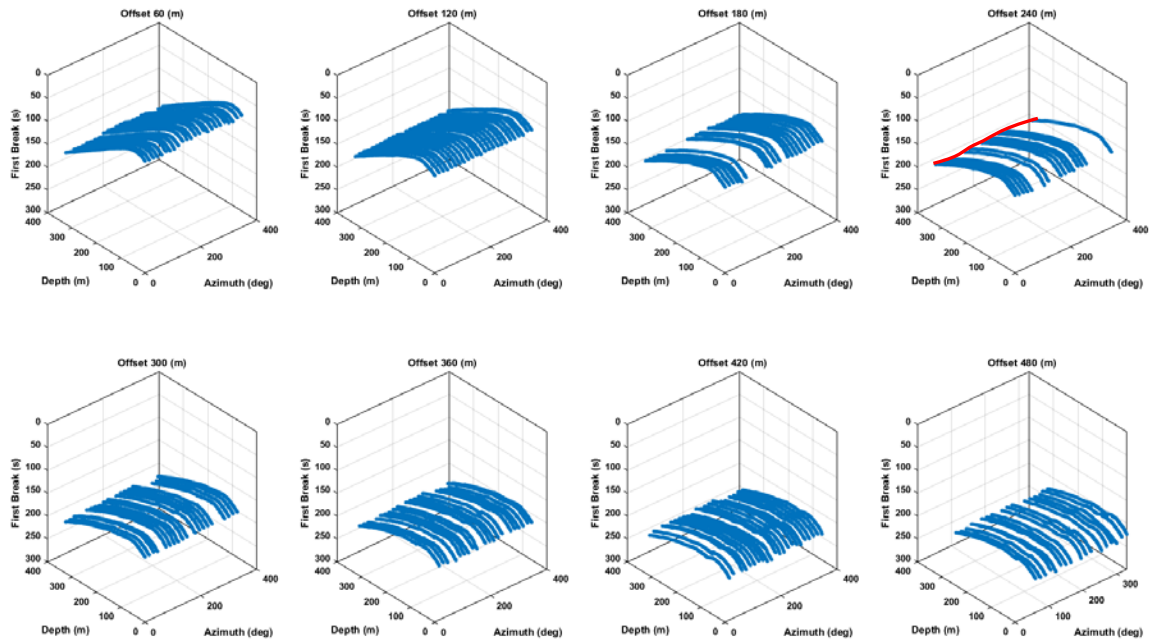


FIG. 9. Offset panels of first break picks after application of 2014 source statics. Sinusoidal patterns are still present, but greatly reduced in amplitude.

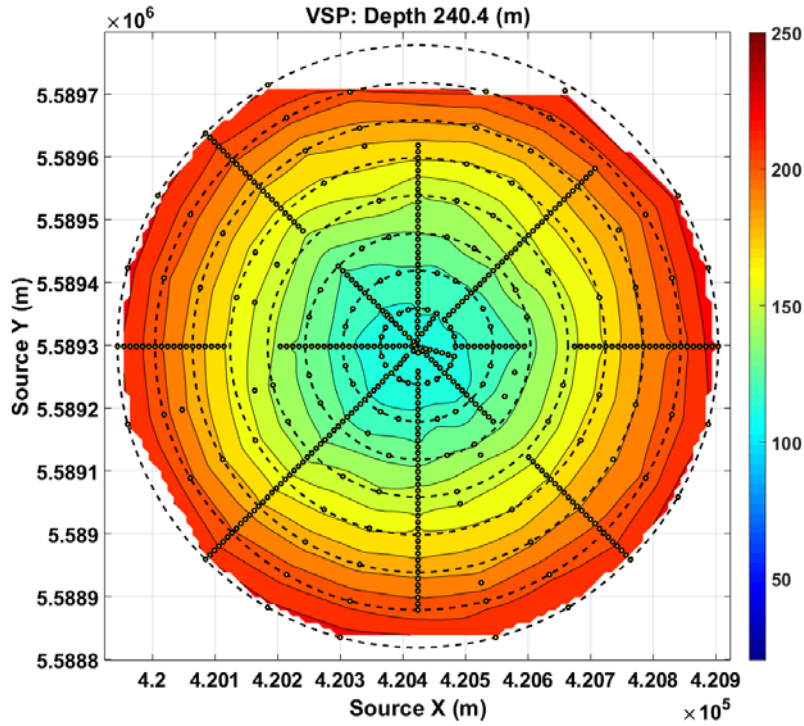


FIG. 10. Contour map of interpolated first break picks positioned at VP locations for receiver at 240 m depth. Non-circular contours may indicate the presence of anisotropy. Black dashed lines are 60 m interval circles centred on the geophysics well.

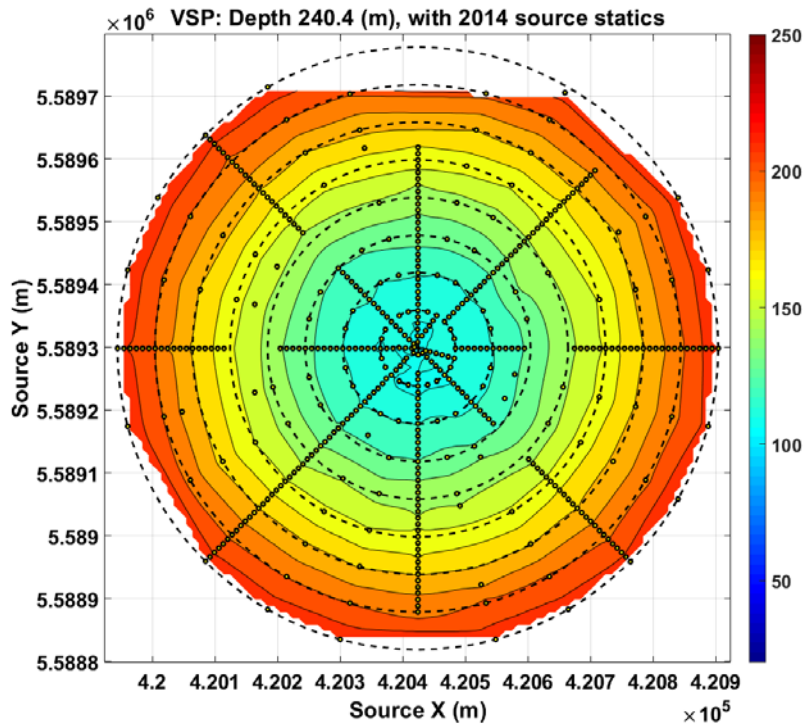


FIG. 11. Contour map of interpolated first break picks positioned at VP locations for receiver at 240 m depth after application of 2014 3C-3D source statics. Black dashed lines are 60 m interval circles centred on the geophysics well.

## FAR OFFSET VSP PROCESSING

Far offset VSP processing has thus far followed examples shown by Hinds et al., (1996) and in the Schlumberger Vista far-offset VSP tutorial. The first step in far offset processing is first-break picking, which was performed on the Vertical (V) component for all VP and used as a guide for the time window used for component rotations. Figures 12 and 13 show examples of the component rotation step for VPs 1151 and 1101, 20 and 480 m from the geophysics well respectively. Blue ellipses on the V panel highlight a polarity reversal which is not seen on VP 1149 data (6 m from the well; Figure 5). The reversal is a multi-trace switch from down-going first motion (trough, or red) at depth to up-going (peak, or black) on shallower traces. This transition moves deeper with increasing source-receiver offset. At this point it is unlikely that first motion on the shallow receivers is a direct-arrival. It is more likely to be a mix of interfering wave-types. Polarity reversals due to horizontal receiver orientation in the borehole are also observed on the H1 and H2 components.

Component rotations from H1 and H2 to Hmax and Hmin (horizontal rotation angle theta; Figure 14), and from V and Hmax to V' and Hmax' (vertical rotation angle phi; Figure 15) were calculated by the Vista module VSPRPol. This module uses a method described by Grechka and Mateeva (2007) to calculate rotation angles using a least-squares minimization algorithm. Initial first-break picking on V transitioned from peak to trough with depth, however, in testing, a horizontal line of picks at the average direct arrival time worked just as well as a guide for VSPRPol for this data (not shown). In addition, polarity reversals observed on Hmin, Hmax and Hmax' are unaffected by reversing polarities on H1 and H2 prior to calling VSPRPol. First-breaks were re-picked on the Hmax' component after one round of manual polarity reversal picking, where we chose to pick polarities so first motion is represented by a trough (red) on Hmax'. It is these picks that are displayed in Figures 8 and 9, and used by Eaid (2018). All traces on the V' panel have been polarity reversed so the polarity of the up-going P wave-field matches the V component.

Rotation angles theta and phi are preserved in the trace headers and were imported into Matlab® in order to plot the source-receiver offset panels shown in Figures 14 and 15, plotted against source-receiver azimuth and receiver depth. Theta shows good consistency with increasing receiver depth, although it starts to spread out a bit more at the farthest offset (480 m, bottom right panel, Figure 14) which correlates with noisier data at depth. It also exhibits wrapping, which may correlate with observed polarity reversals in Hmax and Hmin.

Rotation angle phi exhibits a turn-over that gets wider and moves to greater depths with increasing source-receiver offset. This may correlate with the position of the polarity reversal observed on the vertical component (Figure 15).

Similar to the zero-offset VSP processing, the down-going P wave-field was extracted from Hmax' by flattening on the first-break picks and using a f-k filter (instead of median filter). P-down was then removed from V and Hmax' by subtraction to give us P-up which was then deconvolved using P-down to give us V (decon'd P-up) and Hmax' (decon'd P-up) (left panels; Figures 16 and 17). Ray-tracing using a 1D model constructed from the zero-offset VSP interval velocity curve gives us time-variant rotation angles, which are used for

our final component rotation to  $Z''$  up, mostly containing up-going P wavefield and  $H_{\max}''$  up which mostly contains the up-going  $S_v$  wavefield (right-hand panels; Figures 16 and 17). The velocity curve was constructed using every 10<sup>th</sup> trace, as the Dix equation is unstable for small differences in travel-time. These figures have AGC applied for display, which makes it difficult to compare amplitudes from panel to panel.

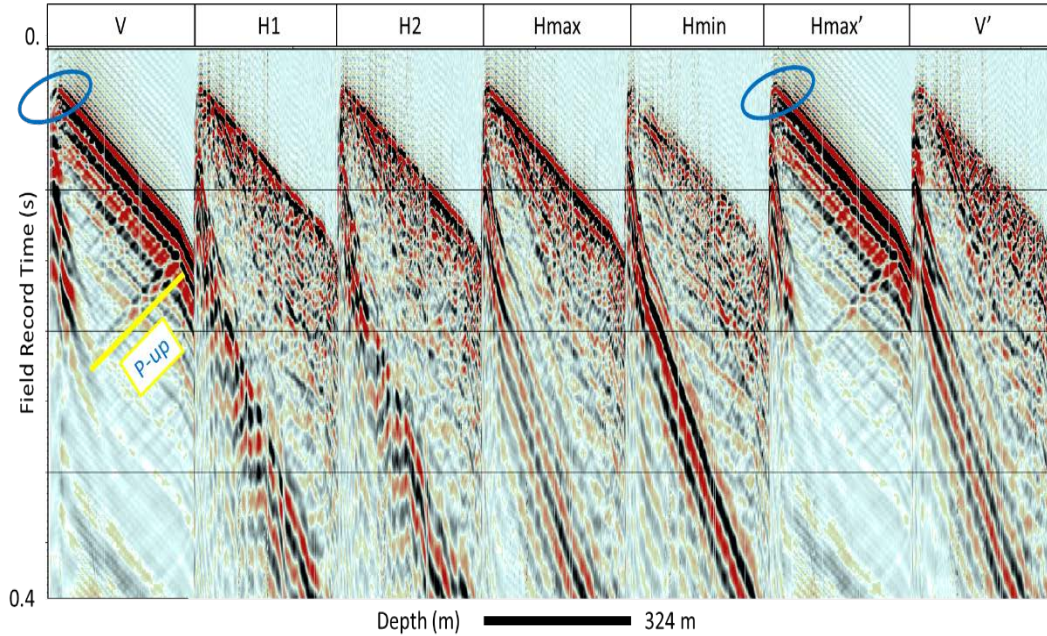


FIG. 12. VP 1151, 20 m offset, component rotation panels.

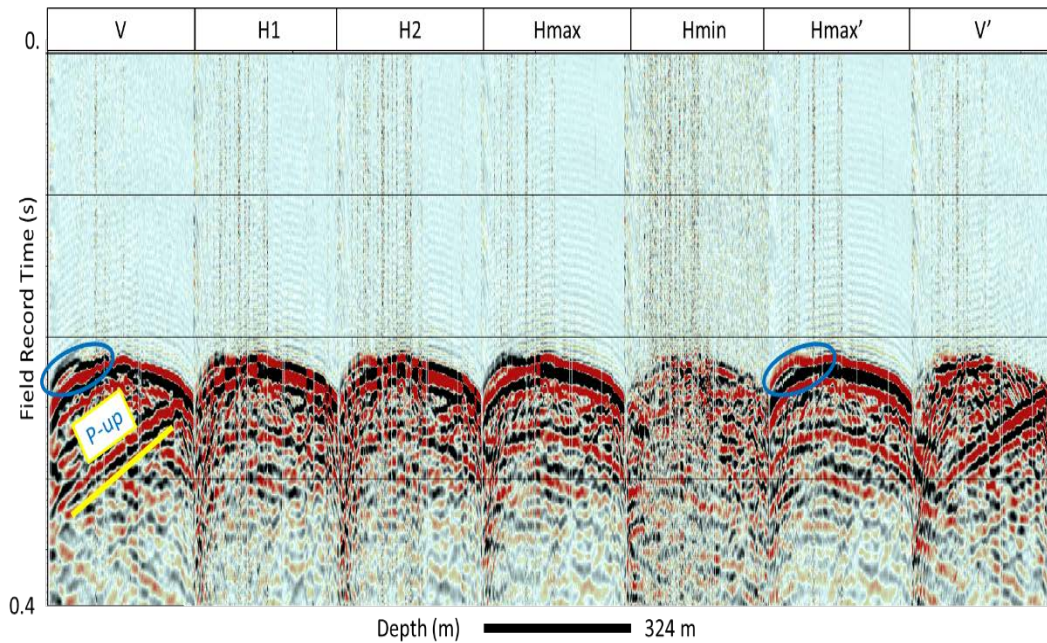


FIG. 13. VP 1101, 480 m offset, component rotation panels.

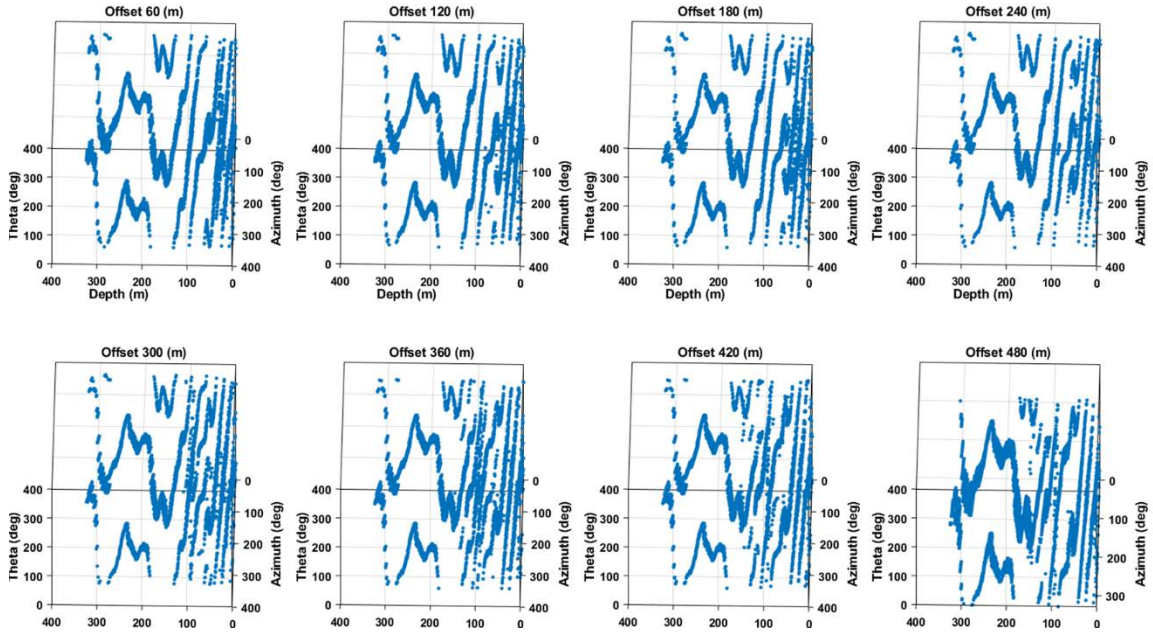


FIG. 14. Offset panels for horizontal rotation angle theta.

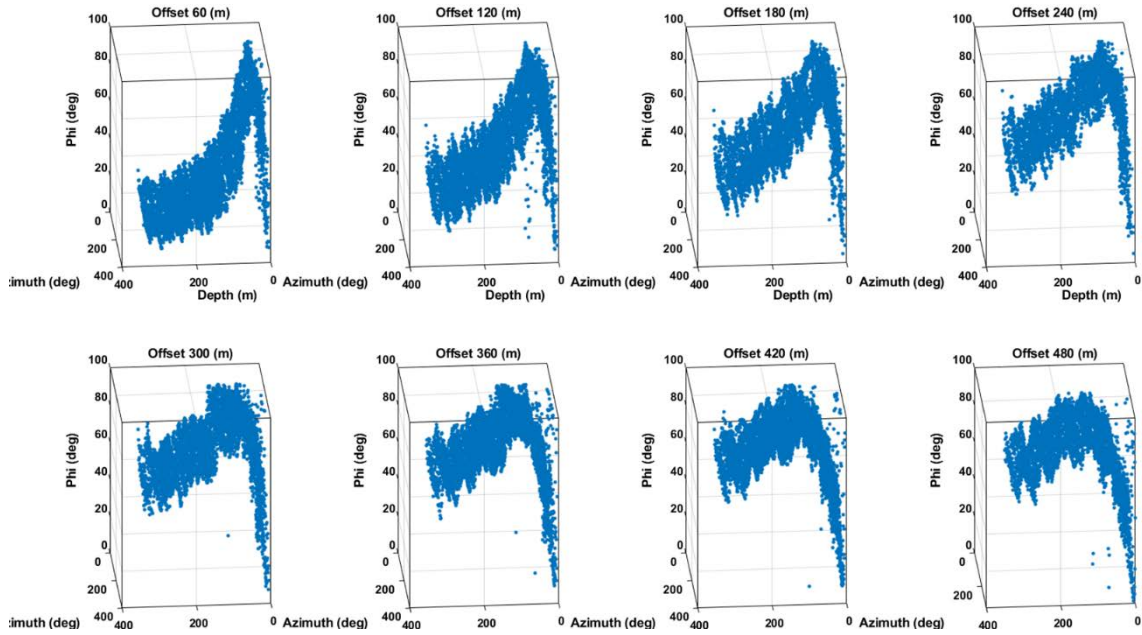


FIG. 15. Offset panels for vertical rotation angle phi.

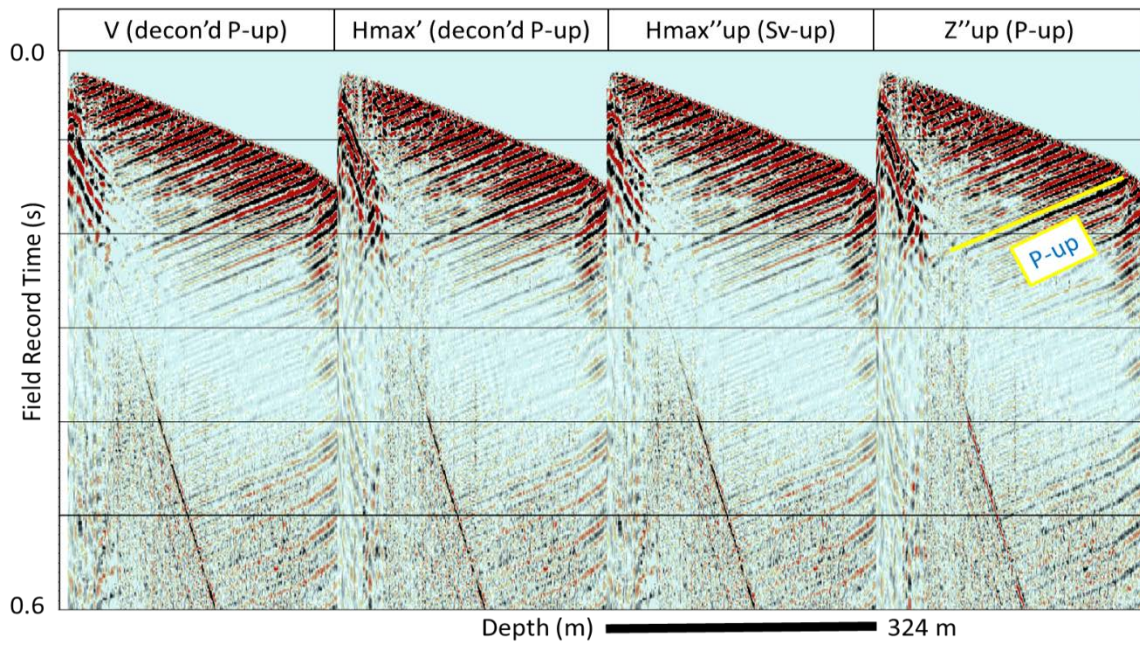


FIG. 16. Time variant rotations to separate upgoing P and upgoing Sv. V and Hmax' were rotated to Hmax''up and Z'' up.

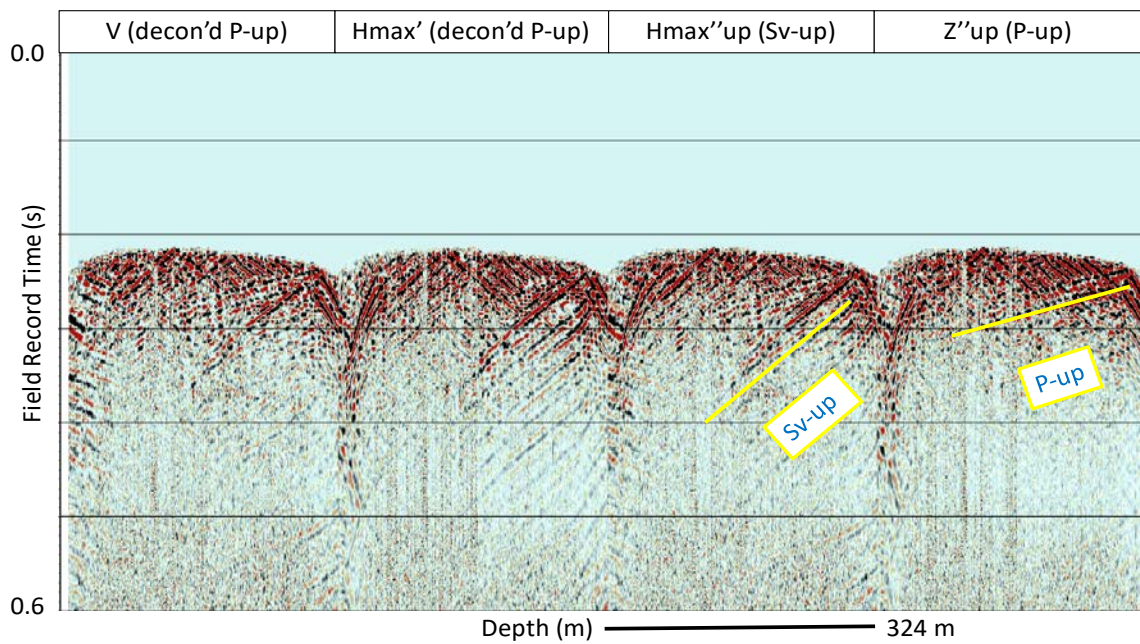


FIG. 17. Time variant rotations to separate upgoing P and upgoing Sv. V and Hmax' were rotated to Hmax''up and Z'' up.

## DISCUSSION AND FUTURE WORK

CREWES acquired a multi-azimuth walk-away VSP at the Containment and Monitoring Institutes Field Research Site (FRS) in Newell County Alberta in September of 2018. Downhole accelerometer data from the geophysics well on the site have been processed to a zero-offset corridor stack that compares well to a P-P synthetic calculated from well logs recorded in the same well. In preparation for future full waveform inversion work, receiver components of far-offset VSP data have been rotated from 1) H1 and H2 (field orientation) to Hmax and Hmin (rotation angle  $\theta$ ), and then V and Hmax to V' and Hmax' (rotation angle  $\phi$ ), where  $\theta$  and  $\phi$  were calculated rather than hand-picked from Hodograms.  $\theta$  shows good consistency with increasing receiver depth, while  $\phi$  shows a turn-over point that appears to track a phase change between up and down-going first motion observed on the vertical component.

First-breaks were initially picked on V, and then re-picked on Hmax'. Analysis of the first-break picks shows that there may be very weak HTI anisotropy present on site, although this finding becomes less convincing after application of source statics from a 3C-3D survey that was conducted in 2014.

The down-going P- wavefield was extracted from the Hmax' component and used to remove down-going P from V and Hmax', which were then deconvolved using the down-going P. Ray-tracing was conducted through a 1D velocity model constructed from the zero-offset velocity curve, and the angles of the rays impinging on receivers in the borehole were used for a further time-variant component rotation from Vup and Hmax'up to Hmax''up and Z''up, where up-going Sv is concentrated on Hmax''up and the up-going P is concentrated on the Z''up component. These results will be the input to future inversions. Z''up has been VSP-CDP transformed and stacked for all source points. However, the results show clear signs of statics problems and are not shown here.

Future work includes (In no particular order), 1) additional processing flow parameter testing and quality control, 2) better well ties and interpretation including comparison to the 2014 3C-3D, 3) use of first-break picks to create a full 3D anisotropic (isotropic?) depth model, 4) completion of far-offset P-P and P-S VSP processing including pre-stack depth migration, 5) comparison to fibre and geophone data from this and other surveys at the FRS and, of course, 6) inversion for physical properties of the Earth.

## ACKNOWLEDGEMENTS

The authors would like to thank (alphabetically) Fotech Solutions, GPUSA, High Definition Seismic Corporation, and Inova Geophysical for field operations, Schlumberger for providing Vista software to the University, and all CREWES sponsors and CaMI.FRS JIP subscribers. This work has been partially funded by NSERC under the grant CRDPJ 461179-13. This research was also supported in part by the Canada First Research Excellence Fund.

## REFERENCES

- Grechka, V. and Mateeva A., 2007, Inversion of P-wave VSP data for local anisotropy: Theory and case study: *Geophysics*, **72**, 4.
- Hall, K., Isaac, H., Wong, J., Bertram, K., Bertram, M., Lawton, D., Bao, X., and Eaton, D., 2015, Initial 3C-2D surface seismic and walkaway VSP results from the 2015 Brooks SuperCable experiment: CREWES Research Report, **27**, 23.
- Hinds, R., Anderson, N., and Kuzmiski, R., 1996, VSP Interpretive Processing: Theory and Practice: Society of Exploration Geophysicists Open File Publications No. 3. ISBN 978-1-56080-042-2.
- Isaac, H., and Lawton, D., 2014, Preparing for experimental CO<sub>2</sub> injection: Seismic data analysis: CREWES Research Report, **26**, 43.
- Macquet M., and Lawton, D., 2018, Ambient noise correlation study at the CaMI Field Research Station, Newell County, Alberta, Canada: CREWES Research Report, this volume.
- Matt Eaid and Kris Innanen, 2018, Toward 4C FWI: DAS and 3C as complementary datasets: CREWES Research Report, this volume.
- Spackman, T., and Lawton, D., 2018, Processing and analysis of data recorded from a buried permanent seismic source: CREWES Research Report, this volume.
- Trad, D., 2018, Compressive sensing, sparse transforms and deblending: CREWES Research Report, this volume.